THE ASTROPHYSICAL JOURNAL, 461:320–326, 1996 April 10

RUNAWAY INSTABILITY OF BLACK HOLE–NEUTRON TORUS SYSTEMS

SHOGO NISHIDA AND YOSHIHARU ERIGUCHI
Department of Earth Science and Astronomy, College of Arts and Sciences, the University of Tokyo, Komaba, Meguro, Tokyo 153, Japan; nishida@valis.c.u-tokyo.ac.jp, eriguchi@tansei.cc.u-tokyo.ac.jp
Received 1995 August 16; accepted 1995 October 11

ABSTRACT

We have obtained fully general relativistic equilibrium configurations of black hole–neutron torus systems and have analyzed their stability. Although several authors have discussed whether such systems can be sources of gamma-ray bursts, their arguments have been based on the qualitative nature of black hole–neutron torus systems because such configurations have not yet been solved. Moreover, since black hole–neutron torus systems are supposed to form after coalescence of binary neutron stars or after collapse of a massive star, a newly formed torus may be in a rather hot state. Therefore we have developed a numerical code that can handle configurations of cold and hot (0.1, 1, and 10 MeV) neutron tori.

Recently, polytropic tori around black holes have been shown to suffer a global runaway instability. As for neutron tori, the self-gravitating tori closely orbiting around the black holes with the mass range of 1–3 $M_\odot$ are destroyed in a timescale $\Delta t_T \ll 1$ s as a result of this instability. This is a much shorter timescale than the evolutionary timescale that is relevant for the current model of gamma-ray bursts based on the merger of binary neutron stars. This result probably excludes the possibility of neutron tori models for gamma-ray bursts as sources at cosmological distances.

Subject headings: accretion, accretion disks — binaries: close — black hole physics — gamma rays: bursts — methods: numerical — stars: neutron

1. INTRODUCTION

Structures of highly relativistic axisymmetric fluid bodies have been solved by several authors (see, e.g., Butterworth & Ipser 1975, 1976; Komatsu, Eriguchi, & Hachisu 1989; Cook, Shapiro, & Teukolsky 1992; Bonazzola et al. 1993). They have been concerned mainly with structures of rotating configurations of a single body or a single star partly because it is the simplest situation for highly relativistic cases and partly because it is the easiest model to solve.

However, from the astrophysical point of view, important phenomena are often related to interactions between two bodies or among several bodies, such as collisions of stars or galaxies, binary systems of stars, star-torus systems, active galactic nuclei consisting of a massive black hole and a surrounding thick accretion disk (see, e.g., Abramowicz, Jaroszyński, & Sikora 1978; Jaroszyński, Abramowicz, & Paczyński 1980; Paczyński & Wiita 1982), and so on.

Furthermore, from a purely general relativistic point of view, the investigation of the effects of surrounding matter on the relativistic bodies such as neutron stars or black holes is a very interesting and challenging problem. If the mass of the surrounding matter cannot be neglected, the central bodies may be significantly affected compared to isolated single bodies. In particular, the central black holes surrounded by massive matter are no longer Kerr-type black holes.

Self-gravitating equilibrium configurations of star-torus systems in general relativity were first obtained by Nishida, Eriguchi, & Lanza 1992), and several gravitational effects of tori on polytropic stars were intensively investigated. Lanza (1992) succeeded in obtaining equilibrium thin disks around black holes. Very recently (Nishida & Eriguchi 1994) we solved the problem of the structure of equilibrium thick tori around black holes. All of these investigations used a polytropic equation of state (hereafter EOS) for the tori. However, in order to study astrophysical phenomena precisely, it is preferable to use more realistic EOSs. In particular, for some situations, the density of the tori will become so high that EOSs for the neutron matter must be included.

In this paper we will investigate compact neutron tori around black holes. This kind of configuration may be formed from interacting binary neutron stars. Neutron stars in a close binary system are considered to spiral in as the angular momentum of the system is being lost via gravitational radiation, and eventually they coalesce.

It is very difficult to simulate the final stage of coalescence. So far, only some particular aspects of this problem have been investigated (see, e.g., Oohara & Nakamura 1992). In most simulations the final stage of coalescence is roughly as follows. A rotating object with the mass of ~ 1–$2\ M_\odot$ appears in the central part and is surrounded by a rotating torus of a comparable but smaller mass. The outer radius of the torus is ~ 100 km. Such a system may also be formed from collapse of a massive rotating star (Woosley 1993; Paczyński 1993). The maximum density inside the torus reaches $\sim 10^{13}$ g cm^{-3}, and the maximum temperature is ≈ 2 MeV. These values are typical for a very hot neutron star. Therefore it is very important to obtain precise equilibrium configurations of tori not only with cool but also with hot neutron matter. In this paper, several EOSs for neutron matter with several constant temperatures (0, 0.1, 1, and 10 MeV) (Lattimer & Swesty 1992) are used to obtain equilibrium tori by extending the numerical scheme of Nishida & Eriguchi (1994).

Moreover, configurations of this type have been discussed in relation to the sources of gamma-ray bursts. Several authors have suggested that gamma-ray bursts may occur in the merger of neutron star binaries (see, e.g., Piran 1993). Gamma-ray bursts had been considered for many years to be associated with compact objects in our Galactic disk. However, after the distribution of more than 150 gamma-ray bursts was detected by the BATSE experiment, it was found that the sources of gamma-ray bursts are distributed isotropically on the sky but not uniformly in the

radial direction (Fishman et al. 1992). This observation suggests that sources of bursts are located at cosmological distances rather than at galactic distances (Murakami et al. 1988).

Hot neutron matter can be a good candidate for a source of gamma-ray bursts because neutrino and antineutrino annihilation may result in gamma rays (see Nishida et al. 1995 for further discussion). However, the efficiency of this mechanism depends strongly on the topology of the neutron matter. It is required that the source region of the gamma rays must be optically thin (see, e.g., Narayan, Paczyński, & Piran 1992). For neutron matter with configuration that is of a spheroidal shape, there occurs a optically thick baryonic wind. In this respect, a toroidal configuration is appropriate for the gamma-ray burst because the centrifugal barrier protects the region near the rotation axis from pollution (see Fig. 1).

However, even for toroidal configurations, it was demonstrated (Nishida et al. 1995) that polytropic tori with the adiabatic index $\gamma = 4/3$ are unstable against the runaway instability proposed by Abramowicz, Calvani, & Nobili (1983). Therefore we need to investigate whether or not the same instability may set in for a realistic torus around a black hole. We will show in the present paper that the runaway instability also exists for cold and hot neutron tori and that because of this instability they survive only for a *much shorter* time than that needed to meet the results of observations of gamma-ray bursts.

In § 2 the basic equations and the numerical scheme to obtain equilibrium solutions are described briefly. The numerical scheme shown here is mainly based on that used by Nishida & Eriguchi (1994). However, in order to obtain realistic neutron tori, some extension from their method is required, and this will be explained. EOSs for neutron tori are also discussed.

In § 3 the runaway instability against axisymmetric mass overflow for neutron tori is investigated. Stability of configurations can be determined by examining equilibrium solutions, i.e., neither normal mode analyses nor numerical simulations are required. The basic concept of the runaway instability and the validity of the method used in the present investigation are explained in detail by Nishida et al. (1995). Although behavior of the instability depends on the choice of EOS, all tori with EOSs for the neutron matter suffer this overflow instability. By investigating the runaway instability of neutron tori, it can be concluded that the black hole–torus model is unlikely to be a candidate for a source of gamma-ray bursts, although it might be the source of other high-energy phenomena.

2. EQUILIBRIUM TORI

In this section we will summarize briefly the basic equations and the numerical scheme for equilibrium structures of a black hole–torus system. As we will apply our equilibrium models of black hole–torus systems to realistic outcome of merging of neutron stars, we choose reasonable but minimum assumptions.

We assume four conditions for the spacetime as follows: the spacetime is (1) stationary, (2) axisymmetric, (3) equatorially symmetric, and (4) asymptotically flat.

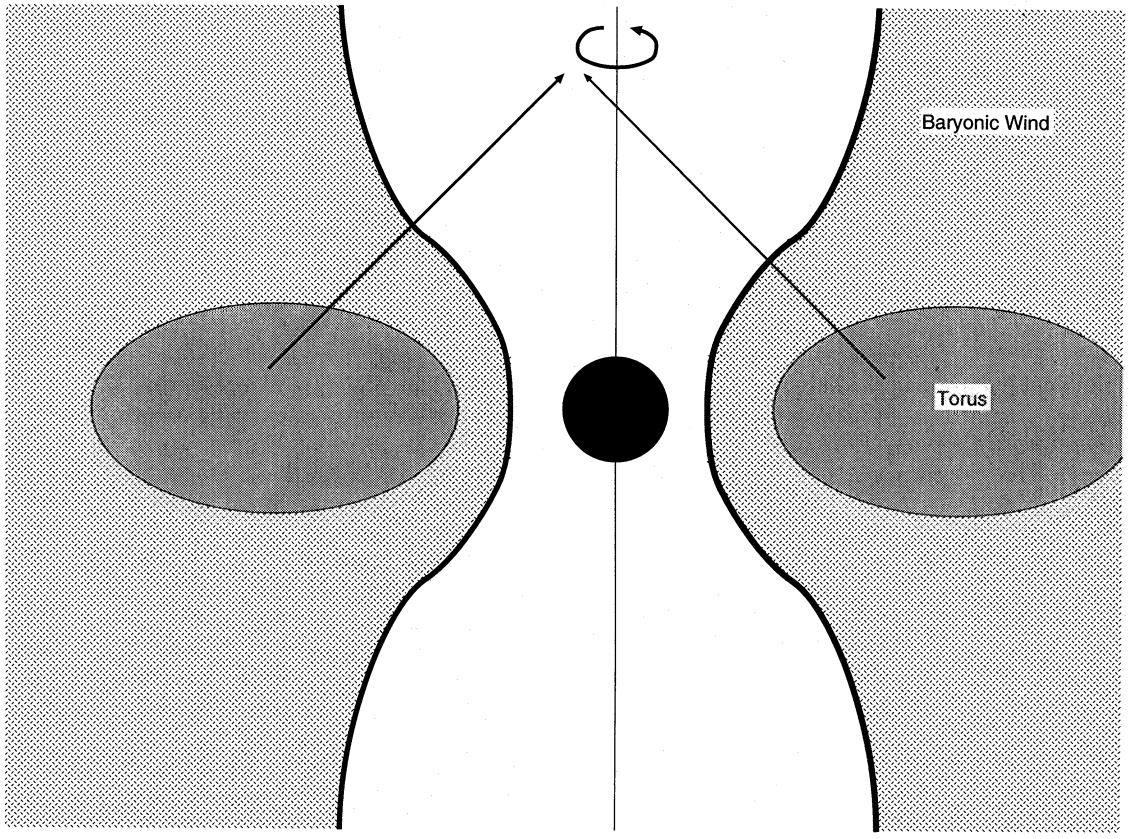

FIG. 1.—A schematic figure of the baryonic wind from a hot torus. The filled circle at the center represents a black hole. Two ellipses are the cross sections of a torus in a meridional plane. The baryonic wind, which is shown by shaded region, cannot reach the rotation axis because of the centrifugal barrier. Thus there exists a baryon-free funnel (*white region*) along the axis. In this funnel, neutrino–antineutrino annihilation to $e^+ e^-$ pairs forms a fireball expanding relativistically, and from this fireball gamma rays are finally emitted.

Under these conditions the metric can be written as

$$ds^2 = -e^{2\nu}dt^2 + e^{2\alpha}(dr^2 + r^2 d\theta^2) + B^2 e^{-2\nu} r^2 \sin^2\theta \times (d\phi - \omega\, dt)^2 , \quad (1)$$

where t and ϕ are the coordinates associated with the timelike and the axial symmetries, respectively. The coordinates r and θ are the radial and the polar coordinates, respectively. Ambiguity of these coordinates can be removed by the requirement of the following relation:

$$g_{rr} = r^2 g_{\theta\theta} . \quad (2)$$

Metric coefficients α, B, ν, and ω are functions depending only on r and θ. The units $c = G = 1$ are chosen throughout this paper. In this coordinate system, assumption 3 can be written as

$$f(\theta) = f(\pi - \theta) , \quad (3)$$

where f is an arbitrary function that is symmetric about the equatorial plane. Assumption 4 means that the matter exists within a finite region near the central part of the coordinate system. From this it follows that

$$\nu \sim -M/r , \quad (4)$$

$$\omega \sim 2J/r^3 , \quad (5)$$

$$B \sim 1 , \quad (6)$$

at a far distance from the center. Here M and J are the total gravitational mass and the total angular momentum of the system, respectively.

Concerning matter, three assumptions are made: it is assumed to be (*a*) perfect fluid, (*b*) barotropic, and (*c*) circularly rotating.

By assumption *a* the stress-energy tensor for the matter, $T^{\mu\nu}$, can be written as

$$T^{\mu\nu} = (\epsilon + p)u^\mu u^\nu + g^{\mu\nu} p , \quad (7)$$

where u^μ, p, and ϵ are the four velocity, the pressure, and the energy density, respectively.

Condition *b* means that the pressure of the matter can be represented as a function of only the baryon mass density of the matter. In this paper, EOSs for neutron matter with several temperatures that satisfy the above condition are used.

For simplicity, we require condition *c*, which means that the matter has only a rotational motion around the rotation axis but no meridional circulation. Thus the four-velocity can be written as follows:

$$u^\mu = \frac{e^{-\nu}}{\sqrt{1 - v^2}} (1, 0, 0, \Omega) , \quad (8)$$

where v is the velocity of a fluid element measured in an inertial frame of a zero angular momentum observer (Bardeen 1973), i.e.,

$$v = (\Omega - \omega) r \sin\theta B e^{-2\nu} . \quad (9)$$

Here Ω is the angular velocity of the fluid measured by an observer at infinity, i.e.,

$$\Omega = \frac{d\phi}{dt} . \quad (10)$$

In stationary, axisymmetric, and circularly rotating models, the existence of a black hole can be expressed in a simple manner (see, e.g., Bardeen 1973). On the event horizon, i.e., on a smooth null hypersurface spanned by two Killing vectors, metric coefficients must behave as follows:

$$B = 0 , \quad (11)$$

$$e^\nu = 0 , \quad (12)$$

$$\omega = \omega_H = \text{constant} , \quad (13)$$

where ω_H is the dragging of the inertial frame on the horizon. It is important to note that the coordinate locus of the horizon can be transformed into a sphere of a constant radius, i.e.,

$$r = h , \quad (14)$$

by keeping the form of equation (1) unchanged (Carter 1973). Here h is a certain constant. These consist of a complete set of boundary conditions on the horizon.

The other boundary condition for the metric comes from the requirement of geometrical regularity at the coordinate singularity, i.e., on the rotation axis. It can be expressed as

$$\alpha = \ln B - \nu , \quad (15)$$

at $\theta = 0$.

Under the assumptions mentioned before, Einstein equations for ν, B, ω, and α can be written straightforwardly. The precise forms of equations for these metric coefficients are not shown here (see Nishida & Eriguchi 1994).

Equations for hydrostatic equilibrium can be written as

$$\nabla p + (\epsilon + p)\left(\nabla \nu - \frac{v}{1 - v^2}\nabla v + \frac{l\nabla\Omega}{1 - l\Omega}\right) = 0 . \quad (16)$$

Here l is the specific angular momentum defined by

$$l = -\frac{u_\phi}{u_t} . \quad (17)$$

In order to obtain equilibrium structures of barotropic stars, a rotation law must be specified. We choose the rotation law that l is constant throughout a torus. By using this rotation law, equation (16) can be integrated into

$$\int \frac{dp}{\epsilon + p} + \nu + \frac{1}{2}\ln(1 - v^2) - \ln(1 - \Omega l) = C , \quad (18)$$

where C is a constant of integration.

The method of calculating solutions is the same as that for black hole–polytropic torus systems, which was described in Nishida & Eriguchi (1994), except that we improved the treatment of EOSs to include neutron equations of state.

It is sufficient to specify only four parameters to obtain a unique solution for neutron tori, although six parameters are needed for polytropes. The difference arises from the fact that there is no need to specify the polytropic index N and the maximum baryon mass density $\rho_{\max}$. The maximum baryon mass density need not be specified, because at each point the mass-energy density distribution ϵ can be obtained without ambiguity from equation (18) and so can be the maximum baryon mass density $\rho_{\max}$. This is in contrast to polytropic cases where only $K^N \rho_{\max}$ can be obtained.

Therefore, four parameters, which must be specified to obtain a unique solution for neutron tori, are chosen as follows:

1. The ratio of the radius of the event horizon h to the outer boundary of the torus r_{out} is $\hat{h} = h/r_{out}$.
2. The dragging of the inertial frame on the horizon is ω_H.
3. The ratio of the radius to the inner boundary of the torus r_{in} to the outer radius is r_{in}/r_{out}.
4. The specific angular momentum of the torus is l.

In the case of neutron tori, since tabulated forms of the EOSs are employed, we cannot follow exactly the same procedure that we used for polytropes. In tables of the EOSs for the neutron matter, discrete values for the energy density, the rest mass density, and the pressure are given. Therefore we have to use some interpolation scheme to evaluate values between data points. We use the piecewise polytropic interpolation scheme (see, e.g., Müller & Eriguchi 1985). We assume that a polytropic relation is satisfied between two neighboring data points. The polytropic constant K and the polytropic index N between two data points are determined by using the equation

$$p = K_i \epsilon^{1+1/N_i} (p_{i-1} \le p < p_i, \epsilon_{i-1} \le 3\epsilon < \epsilon_i) . \quad (19)$$

Here K_i and N_i are corresponding values between $(i-1)$th and ith points and are determined from data at two neighboring points.

Consequently the integration of the first term of the left-hand side of equation (18) from zero to ϵ becomes

$$\sum_{i=1}^{m} [\ln(K_i \epsilon_i^{1/N_i} + 1) - \ln(K_i \epsilon_{i-1}^{1/N_i} + 1)] + \ln(K_{m+1} \epsilon^{1/N_{m+1}} + 1) - \ln(K_{m+1} \epsilon_m^{1/N_{m+1}} + 1) \times (\epsilon_m \le \epsilon < \epsilon_{m+i}) . \quad (20)$$

In this paper four types of EOSs for the neutron matter are used for our calculations. Their density-pressure relations are plotted in Figure 2. The EOS for 0 MeV is that of Bethe & Johnson (1974), and EOSs for 0.1, 1, and 10 MeV are those calculated by Lattimer & Swesty (1992) for constant temperatures. It is obvious that the hotter the neutron matter becomes, the higher the pressure tends to be for the same energy density. The higher pressure implies that structures of equilibrium configuration may be significantly changed for the hot states because equilibrium states are achieved by the balance of the three forces, i.e., the gravitation, the centrifugal force, and the pressure gradient. Thus, if the maximum pressure at the center is the same for different equilibrium models, neutron tori with higher temperature must have a lower maximum density.

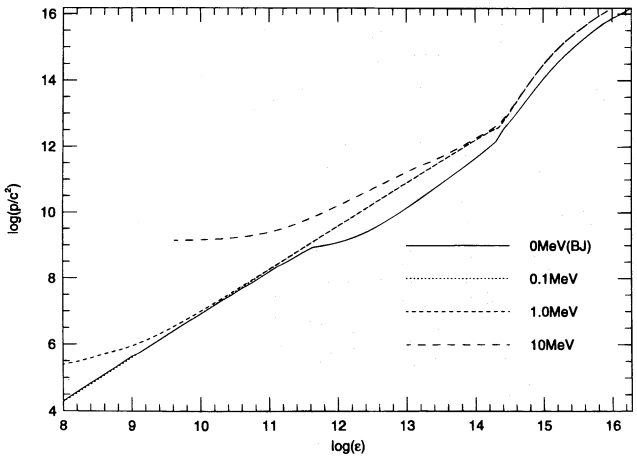

FIG. 2.—The pressure p/c^2 is plotted against the energy mass density ϵ for four EOSs. The EOS for 0 MeV is obtained by Bethe & Johnson (1974), and the EOSs for 0.1, 1, and 10 MeV are calculated by Lattimer & Swesty (1992) under the assumption of constant temperature. However, since there is no data for the range below $\rho \sim 10^9$ g cm^{-3} for the EOS of 10 MeV, a polytropic EOS is used to fit the leftmost boundary of the 10 MeV data for the calculations of this paper. In this figure, lines of 0 and 0.1 MeV overlap each other in the region 10^8 g cm$^{-3} \lesssim \rho \lesssim 10^{11}$ g cm^{-3}. The same thing occurs for 0.1 and 1 MeV in the region 10^{11} g cm$^{-3} \lesssim \rho \lesssim 10^{14}$ g cm^{-3} and for 0.1, 1, and 10 MeV in the region 10^{14} g cm$^{-3} \lesssim \rho \lesssim 10^{16}$ g cm^{-3}. As seen from this figure, for the same density, the higher the temperature of the neutron matter becomes, the higher the pressure tends to be.

3. RUNAWAY INSTABILITY

In this section we will analyze the axisymmetric stability of the black hole–torus system against mass overflow. We will show that massive tori are unstable against mass overflow. This was described as runaway instability by Abramowicz et al. (1983). It should be noted that in this runaway instability the relativistic Roche lobe overflow plays a key role. As mentioned before, the basic concept of the runaway instability is explained and an analysis for a black hole–polytropic torus system is given in Nishida et al. (1995). The difference between a polytropic torus and a neutron torus in analyzing the runaway instability is that there are four parameters to be specified for a neutron torus, although five for a $\gamma = 4/3$ polytropic torus. This does not mean that a neutron torus is easier to investigate than a polytropic torus, because there are no scaling parameters that can be specified freely for a neutron torus. For the analysis of the runaway instability, the most practical choice of these four physical parameters is as follows:

total gravitational mass of the system $= M$,

total angular momentum of the system $= J$,

gravitational mass of the black hole $= M_h$,

and

angular momentum of the black hole $= J_h$.

Since the total mass and the total angular momentum are conserved during an axisymmetric accretion, we have

$$\delta M = 0 \quad (21)$$

and

$$\delta J = 0 . \quad (22)$$

Furthermore, the change of the mass and the change of the angular momentum of the black hole must satisfy the following relation:

$$\delta J_h = l \, \delta M_h . \quad (23)$$

The runaway instability can be analyzed in a four-dimensional abstract space as is done for polytropic tori (Nishida et al. 1995). This is because one equilibrium configuration can be represented by four physical quantities: M, J, M_h, and J_h, i.e., a point in this four-dimensional space. In this space, we need to investigate only a two-dimensional surface, $\mathscr{S}$, determined from conditions (21) and (22). On this surface, there is a critical curve, $\mathscr{R}$, which consists of critical configurations. Here critical configurations are those equilibrium states in which the matter of the torus fills up its Roche lobe. Equilibrium states exist

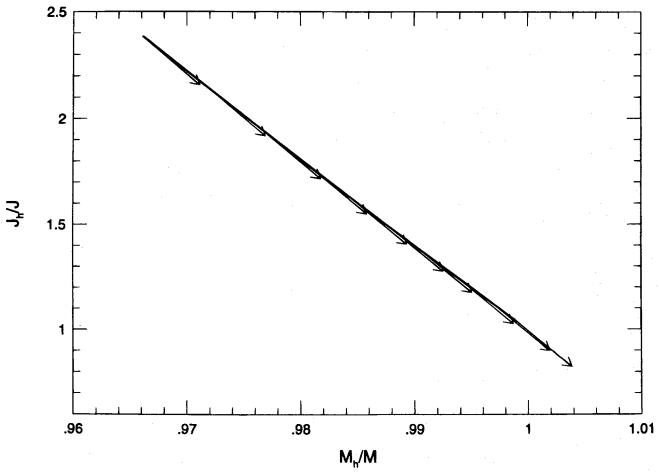

FIG. 3.—The locus $\mathscr{R}$ of critical equilibrium configurations for 0.1 MeV tori is shown in the (J_h/J)–(M_h/M) plane, which is a surface in the four-dimensional parameter space sliced by $M = 2.8\ M_\odot$ and $J = -6.0 \times 10^{48}$ g cm^2 s^{-1}, where the geometrical units, $c = G = 1$, are used. All the equilibrium configurations lie above the curve $\mathscr{R}$. Virtual configurations for which mass overflows the Roche lobe lie below the curve $\mathscr{R}$. The arrows represent the direction of the evolutionary response of critical configurations to infinitesimal mass transfer. Directions of the arrows indicate that all the critical equilibrium configurations shown in the figure are unstable against the mass overflow.

only above this critical curve. Thus there are no equilibrium configurations under the critical curve. We will call this region a forbidden region.

Condition (23) determines a direction of evolution of the system once an accretion begins. If this direction is toward the forbidden region, the critical solution considered is unstable against the runaway instability. In other words, by comparing the value of the slope of the critical curve, i.e.,

$$\Theta \equiv \left(\frac{\partial J_h}{\partial M_h}\right)_{M,J}, \tag{24}$$

and the value of l, we can determine whether the critical model is stable or not.

In Figure 3, the surface $\mathscr{S}$ of 0.1 MeV models is shown. As seen from this figure, all calculated models are unstable, i.e., the runaway instability occurs for all models on the critical line. Results for tori with 0, 0.1, and 1.0 MeV neutron EOSs are given in Tables 1–3. In these tables, M_{tr} and J_{tr} are the gravitational mass and the angular momentum of the torus, respectively. As seen from these tables, all calculated models, irrespective of the temperature, are unstable against the mass overflow. Furthermore, the value of $|l/\Theta|$ increases as the mass of the tori decreases. This behavior is different from that of polytropic tori (Nishida et

TABLE 1

CRITICAL MODELS FOR NEUTRON TORI WITH 0 MEV

M_{tr}	J_{tr}/J	r_{out}	$\lvert l\rvert$	$\lvert\Theta\rvert$	$\lvert l/\Theta\rvert$
$M = 2.0\ M_\odot$, $J = 8.0 \times 10^{48}$ g cm^2 $^{-1}$					
4.279E−02.....	2.884E−01	3.991E+06	1.570E+01	1.355E+01	1.159E+00
2.623E−02.....	1.762E−01	3.896E+06	1.568E+01	1.349E+01	1.162E+00
1.573E−02.....	1.053E−01	3.800E+06	1.566E+01	1.340E+01	1.169E+00
3.211E−03.....	2.146E−02	3.525E+06	1.561E+01	1.342E+01	1.163E+00
8.194E−04.....	5.419E−03	3.135E+06	1.554E+01	1.329E+01	1.169E+00
2.426E−04.....	1.585E−03	2.820E+06	1.548E+01	1.312E+01	1.180E+00
6.859E−05.....	4.429E−04	2.562E+06	1.542E+01	1.294E+01	1.192E+00
4.797E−06.....	3.032E−05	2.163E+06	1.532E+01	1.266E+01	1.210E+00
2.579E−07.....	1.599E−06	1.871E+06	1.522E+01	1.243E+01	1.225E+00
5.535E−08.....	3.399E−07	1.753E+06	1.518E+01	1.229E+01	1.235E+00
1.833E−09.....	1.106E−08	1.556E+06	1.511E+01	...	...
$M = 2.0\ M_\odot$, $J = 1.0 \times 10^{46}$ g cm^2 s^{-1}					
1.086E−02.....	6.349E+01	4.639E+06	1.333E+04	1.171E+04	1.139E+00
6.676E−03.....	3.901E+01	4.507E+06	1.331E+04	1.172E+04	1.136E+00
1.863E−03.....	1.080E+01	4.025E+06	1.326E+04	1.160E+04	1.143E+00
3.757E−05.....	2.100E−01	2.903E+06	1.310E+04	1.119E+04	1.170E+00
1.655E−06.....	9.040E−03	2.414E+06	1.300E+04	1.097E+04	1.185E+00
6.157E−07.....	3.343E−03	2.298E+06	1.297E+04	...	...

TABLE 2

CRITICAL MODELS FOR NEUTRON TORI WITH 0.1 MEV

M_{tr}	J_{tr}/J	r_{out}	$\lvert l\rvert$	$\lvert\Theta\rvert$	$\lvert l/\Theta\rvert$
$M = 2.8\ M_\odot$, $J = 7.0 \times 10^{49}$ g cm^2 s^{-1}					
2.326E+00.....	1.023E+00	1.874E+06	1.541E+00	8.000E−01	1.926E+00
2.314E+00.....	1.020E+00	1.867E+06	1.547E+00	7.766E−01	1.992E+00
2.301E+00.....	1.016E+00	1.860E+06	1.554E+00	8.000E−01	1.942E+00
2.285E+00.....	1.011E+00	1.852E+06	1.561E+00	...	...
$M = 2.8\ M_\odot$, $J = 5.0 \times 10^{48}$ g cm^2 s^{-1}					
6.504E−02.....	1.075E+00	7.841E+06	5.176E+01	4.711E+01	1.099E+00
5.358E−02.....	8.825E−01	7.586E+06	5.169E+01	4.704E+01	1.099E+00
4.431E−02.....	7.269E−01	7.341E+06	5.161E+01	4.672E+01	1.105E+00
3.632E−02.....	5.935E−01	7.109E+06	5.154E+01	...	...

TABLE 3

CRITICAL MODELS FOR NEUTRON TORI WITH 1.0 MeV [a]

M_{tr}	J_{tr}/J	r_{out}	$\|l\|$	$\|\Theta\|$	$\|l/\Theta\|$
9.366E−02.....	1.596E+00	1.480E+07	5.265E+01	4.785E+01	1.100E+00
7.591E−03.....	1.250E−01	9.828E+06	5.202E+01	4.618E+01	1.126E+00
5.332E−04.....	8.601E−03	7.712E+06	5.165E+01	4.519E+01	1.143E+00
4.423E−05.....	7.091E−04	6.723E+06	5.144E+01	4.483E+01	1.147E+00
3.959E−06.....	6.430E−05	5.783E+06	5.117E+01	...	...

[a] $M = 2.8\,M_\odot$, $J = 7.0 \times 10^{49}$ g cm^2 s^{-1}.

al. 1995). Therefore neutron tori are always unstable irrespective of their mass. This implies that a neutron torus around a black hole that fills its Roche lobe will fall into the black hole in a dynamical timescale, i.e., $\sim 10^{-4}$ s, which is $\sim 10^5$–10^6 times shorter than that required to be a source of a gamma-ray burst.

4. DISCUSSION

We have shown that all our calculated models are unstable. For neutron tori, their instability is excited by several different mechanisms. This situation is different from that for polytropic tori (Nishida et al. 1995). Here we will discuss how the neutron tori becomes unstable and what mechanism is the main cause of instability during the accretion process. Comparing carefully the results of Abramowicz et al. (1983) and Wilson (1984) with ours, we find that there are four key factors on which the criterion of the runaway instability depends.

The first factor is the self-gravity of the torus. Abramowicz et al. (1983) have calculated models, some of which are self-gravitating and others of which are non–self-gravitating, and they have shown that inclusion of self-gravity makes tori more unstable. This tendency can be easily explained as follows. The self-gravity of the torus is likely to bind itself tightly by its gravitational force so that the innermost surface of the torus gets closer to the density maximum point of the torus, i.e., moves outward. On the other hand, the cusp is pushed away toward the black hole by the gravitational force of the torus. When a small fraction of the mass of the torus falls onto the black hole, the gravitational force of the torus decreases and the gravity of the black hole increases. This means that the surface of the torus expands or moves closer to the black hole and that the cusp moves closer to the torus compared to non–self-gravitating models. Thus a self-gravitating torus is more unstable than a non-self-gravitating one.

The second factor is the mass ratio of the torus to the black hole. It should be noted that even if we consider the mass of the torus, we may treat it as if it is a non–self-gravitating body. Here we neglect the self-gravity of the torus when we refer to the mass ratio of the torus to the black hole. For polytropic models of Abramowicz et al. (1983) and Nishida et al. (1995), the torus becomes unstable when the mass ratio increases. Although in the models of Wilson (1984) there are no unstable tori, it has still been shown that models tend to approach an unstable region when the mass ratio is increased. When a non–self-gravitating polytropic torus loses its mass, it is obvious that the torus shrinks irrespective of its polytropic index. The cusp moves toward the torus because of the increase of the gravitational force of the black hole (here it should be noted that the gravity of the mass fallen to the black hole is considered to be self-gravitating in Wilson's models). Thus the cusp and the innermost surface of the torus behave qualitatively in the same way whatever the mass ratio of the initial critical equilibrium is. The stability depends on the location of the cusp of the critical model. If it is closer to the marginally stable orbit or if the mass ratio is small, then the critical torus becomes smaller. When the torus loses its mass, the torus shrinks faster than the cusp moves, and so the torus becomes stable.

The third factor is the spin-up of the black hole. As discussed by Wilson (1984), when the angular velocity of the black hole increases, the cusp moves toward the black hole and the torus is stabilized. Although Wilson (1984) concluded that this effect plays the most significant role in the accretion process, it has been shown by our results that there are still unstable models even if we include the effect of spin-up.

In Table 4 we summarize the relation between three key factors and qualitative results of different authors, including us. From this table it can be seen that the order of importance of the three factors is as follows:

$$\text{self-gravity} > \text{spin-up} > \text{mass ratio up}\ .$$

We cannot tell how important is the softness of matter—the fourth factor—by comparing it with other factors. However, we can see that the softness of the matter should be deeply related to the instability from the difference between the results of the $\gamma = 4/3$ polytropic tori and the neutron tori as shown in the previous section.

The softness of the matter can be expressed effectively by a polytropic index N. For polytropic tori, Abramowicz et al.

TABLE 4

BASIC FACTORS INCLUDED IN THE RUNAWAY INSTABILITY ANALYSIS BY SEVERAL AUTHORS

Factor	Abramowicz et al. 1983	Wilson 1984	Nishida et al. 1995	Present Results
Stability.....	Unstable	Stable	Unstable	Unstable
Self-gravity	Yes/no	No	Yes	Yes
M_t/M change	Yes	Yes	Yes	Yes
BH spin change.....	No	Yes	Yes	Yes
$N > 3$	No	No	No	Yes

NOTE.—"Yes" means that the factor is included. "No" means that the factor is not included. "Yes/no" means that the factor is included for some models and is not included for other models.

(1983), Wilson (1984), and Nishida et al. (1995) have investigated only $N = 3$ polytropes so that it seems to be of no use to argue about the effect of the polytropic index. However, it is possible to explain the results for the neutron tori by assuming that neutron tori have some typical effective polytropic index that can be used to discuss the runaway instability. To study the effect of the polytropic index, we have calculated equilibrium models of Newtonian tori with various polytropic indices by using the pseudo-Newtonian potential (see, e.g., Abramowicz et al. 1983). By investigating these models, we found that polytropes with larger N are more unstable. Since the tori with the EOSs for neutron matter have regions where the effective polytropic index is larger than 3, it is natural that all neutron tori are unstable.

All investigations of the runaway instability of tori are restricted to models with constant angular momentum distribution, so we cannot argue about effects by means of the change of the angular momentum distribution. They may be argued in our future investigations.

This paper is based on the first author's (S. N.) Ph.D. thesis, which was submitted to the University of Tokyo in partial fulfillment of the requirements of the doctorate. We would like to express our gratitude to A. Lanza, with whom we enjoyed useful discussions of the runaway instability. We would also like to thank M. A. Abramowicz for his suggestion to apply our numerical code to the astrophysical phenomena.

REFERENCES

Abramowicz, M. A., Calvani, M., & Nobili, L. 1983, Nature, 302, 597
Abramowicz, M. A., Jaroszyński, M., & Sikora, M. 1978, A&A, 63, 221
Bardeen, J. M. 1973, in Black Holes, ed. B. DeWitt & C. DeWitt (New York: Gordon & Breach), 241
Bethe, H. A., & Johnson, M. 1974, Nucl. Phys., A, 230, 1
Bonazzola, S., Gourgoulhon, E., Salgado, M., & Marck, J. A. 1993, A&A, 278, 421
Butterworth, J. M., & Ipser, J. R. 1975, ApJ, 200, L103
———. 1976, ApJ, 204, 200
Carter, B. 1973, in Black Holes, ed. B. DeWitt & C. DeWitt (New York: Gordon & Breach), 125
Cook, G. B., Shapiro, S. L., & Teukolsky, S. A. 1992, ApJ, 398, 203
Fishman, G. J., et al. 1992, ApJS, 92, 229
Jaroszyński, M., Abramowicz, M. A., & Paczyński, B. 1980, Acta Astron., 30, 1
Komatsu, H., Eriguchi, Y., & Hachisu, I. 1989, MNRAS, 237, 355
Lanza, A. 1992, ApJ, 389, 141
Lattimer, J. M., & Swesty, F. D. 1992, Nucl. Phys., A535, 331
Müller, E., & Eriguchi, Y. 1985, A&A, 12, 32
Murakami, T., Fujii, M., Hayashida, K., Itoh, M., & Nishimura, J. 1988, Nature, 335, 234
Narayan, R., Paczyński, B., & Piran, T. 1992, ApJ, 395, L83
Nishida, S., & Eriguchi, Y. 1994, ApJ, 427, 429
Nishida, S., Eriguchi, Y., & Lanza, A. 1992, ApJ, 401, 618
Nishida, S., Lanza, A., Eriguchi, Y., & Abramowicz, M. A. 1995, MNRAS, submitted
Oohara, K., & Nakamura, T. 1992, Prog. Theor. Phys., 88, 307
Paczyński, B. 1993, Princeton Obs. preprint
Paczyński, B., & Wiita, P. J. 1982, A&A, 88, 23
Piran, T. 1993, Sci. Am., 272, 34
Wilson, D. B. 1984, Nature, 312, 620
Woosley, S. E. 1993, ApJ, 405, 273